THE JOURNAL OF BIOLOGICAL CHEMISTRY VOL. 284, NO. 31, pp. 21077–21089, July 31, 2009

Dual 12/15- and 5-Lipoxygenase Deficiency in Macrophages Alters Arachidonic Acid Metabolism and Attenuates Peritonitis and Atherosclerosis in ApoE Knock-out Mice*[S]

Received for publication, March 30, 2009, and in revised form, May 22, 2009 Published, JBC Papers in Press, June 9, 2009, DOI 10.1074/jbc.M109.000901

Daniel Poeckel[‡], Karin A. Zemski Berry[§], Robert C. Murphy[§], and Colin D. Funk[‡1]

From the [‡]Departments of Physiology and Biochemistry, Queen's University, Kingston, Ontario K7L 3N6, Canada and the [§]Cell Biology Division and Department of Pharmacology, University of Colorado Denver, Aurora, Colorado 80045

Lipoxygenase (LO) enzymes catalyze the conversion of arachidonic acid (AA) into biologically active lipid mediators. Two members, 12/15-LO and 5-LO, regulate inflammatory responses and have been studied for their roles in atherogenesis. Both 12/15-LO and 5-LO inhibitors have been suggested as potential therapy to limit the development of atherosclerotic lesions. Here we used a genetic strategy to disrupt both 12/15-LO and 5-LO on an apolipoprotein E (apoE) atherosclerosis-susceptible background to study the impact of dual LO blockade in atherosclerosis and inflammation. Resident peritoneal macrophages are the major cell type that expresses both LO enzymes, and we verified their absence in dual LO-deficient mice. Examination of AA conversion by phorbol myristate acetate-primed and A23187-challenged macrophages from dual LO-deficient mice revealed extensive accumulation of AA with virtually no diversion into the most common cyclooxygenase (COX) products measured (prostaglandin E_2 and thromboxane B_2). Instead the COX-1 by-products 11-hydroxy-eicosatetraenoic acid (HETE) and 15-HETE were elevated. The interrelationship between the two LO pathways in combination with COX-1 inhibition (SC-560) also revealed striking patterns of unique substrate utilization. 5-LO- and dual LO-deficient mice exhibited an attenuated response to zymosan-induced peritoneal inflammation, emphasizing roles for 5-LO in regulating vascular permeability. We observed gender-specific attenuation of atheroma formation at 6 months of age at both the aortic root and throughout the entire aorta in chow-fed female dual LO-deficient mice. We propose that some of the inconsistent data obtained with single LO-deficient mice could be attributable to macrophage-specific patterns of altered AA metabolism.

Lipoxygenase (LO)[2] enzymes are an important source of lipid mediators throughout the plant and animal kingdoms (1, 2). In mammals, these mediators are predominantly formed from arachidonic acid (AA) and act in various physiological and pathological contexts (1–3). Accordingly 5-LO and 12/15-LO are two members of the LO family involved in cardiovascular and inflammatory diseases expressed to variable degrees in several cell types of the myeloid lineage, and their expression is strictly regulated and incompletely understood (2, 4, 5). Despite considerable structural homology between 5-LO and 12/15-LO, both enzymes generate distinct products. The 5-LO metabolite leukotriene (LT) A_4 is precursor to the proinflammatory LTB_4 and cysteinyl LTs, which regulate leukocyte subset-specific chemotaxis (LTB_4) and vascular permeability (cysteinyl LTs), both crucial events during acute peritonitis (1, 6, 7). 12- and 15-HETE, end products synthesized by 12/15-LO, play potential roles in cellular chemotaxis, cancer growth, and inflammation (2, 8). Transcellular interaction products derived from both 12/15-LO and 5-LO, such as lipoxins and maresins, indicate that these enzymes can possess anti-inflammatory activities in innate immunity and the resolution of inflammation (9, 10).

In mice, only one cell type is known to express substantial quantities of both 5-LO and 12/15-LO, the peritoneal macrophage (PMΦ) (2, 11, 12). However, differences in subcellular localization, trafficking, and activation (8, 12–16) of these two LOs indicate that they are independently regulated and not functionally coupled. Tissue-resident MΦ (such as PMΦ) represent the first line of defense against invading pathogens and activate the immunological and inflammatory response (17). These phagocytes are capable of elaborating a wide spectrum of bioactive lipid mediators from the LO and cyclooxygenase (COX) pathways. Little is known about the regulation and putative interdependence of these pathways. Some insight was

* This work was supported, in whole or in part, by National Institutes of Health Grant GM069338 from the NIGMS, LipidMaps. This work was also supported by German Research Foundation (Deutsche Forschungsgemeinschaft) Postdoctoral Fellowship PO 1308/1 (to D. P.) and Canadian Institutes of Health Research Grant MOP-67146 (to C. D. F.).

[S] The on-line version of this article (available at http://www.jbc.org) contains supplemental Figs. 1 and 2.

[1] Holds a Tier I Canada Research Chair in Molecular, Cellular and Physiological Medicine and recipient of a Career Investigator Award from the Heart and Stroke Foundation of Ontario. To whom correspondence should be addressed: Dept. of Physiology, Queen's University, Botterell Hall, Kingston, Ontario K7L 3N6, Canada. Tel.: 613-533-3242; Fax: 613-533-6880; E-mail: funkc@queensu.ca.

[2] The abbreviations used are: LO, lipoxygenase; AA, arachidonic acid; COX, cyclooxygenase; HETE, hydroxyeicosatetraenoic acid; LDL, low density lipoprotein; nLDL, native low density lipoprotein; AcLDL, acetylated low density lipoprotein; LT, leukotriene; MΦ, macrophage(s); PG, prostaglandin; PMΦ, peritoneal macrophage(s); res-PMΦ, resident peritoneal macrophage(s); SBR, spleen/body weight ratio; TGL, thioglycollate; Tx, thromboxane; apoE, apolipoprotein E; 12+5+, 12/15-$LO^{+/+}$ 5-$LO^{+/+}$; 12+5−, 12/15-$LO^{+/+}$ 5-$LO^{-/-}$; 12−5+, 12/15-$LO^{-/-}$ 5-$LO^{+/+}$; 12−5−, 12/15-$LO^{-/-}$ 5-$LO^{-/-}$; wt, wild type; TG, triglyceride; HDL, high density lipoprotein; PBS, phosphate-buffered saline; TGL-PMΦ, TGL-elicited PMΦ; UPLC, Ultra-Performance Liquid Chromatography; LC-MS/MS, liquid chromatography-tandem mass spectrometry.

gained using mice lacking 12/15-LO where substrate shunting from the 12/15-LO into the 5-LO pathway was observed (12).

The generation of knock-out mice for 12/15-LO (12) and 5-LO (18) has enabled the study of these lipid mediator pathways in models of health and disease. Because 12/15-LO and 5-LO are primarily expressed in distinct hematopoietic cells, their implication in various inflammatory disorders and models of host defense mechanisms have been investigated (2, 3). Atherosclerosis, an inflammatory disease prevalent in societies with high dietary fat intake, is initiated by low density lipoprotein (LDL) retention in the vascular wall (19) and subsequent oxidative modification. This process greatly enhances the LDL atherogenic potential, and intriguingly 12/15-LO can contribute to lipoprotein oxidation (11, 20). Initial studies using 12/15-LO- and 5-LO-deficient mice indicated proatherogenic roles for these enzymes (20, 21). Additionally mice lacking the LTB_4 receptor BLT-1 exhibit protection in early atherogenesis (22), but subsequent data from our laboratory using 5-LO-deficient mouse models have not supported an involvement of 5-LO in atherogenesis (3, 23, 24). Here we studied the consequences of simultaneous 12/15-LO and 5-LO knock-out on peritoneal inflammation and atherosclerosis in apoE-deficient mice and surmised whether some of the capricious results in atherosclerotic lesion studies could be attributable to variable eicosanoid profiles.

EXPERIMENTAL PROCEDURES

Animals and Procedures—12/15-LO-deficient, 5-LO-deficient, and apoE-deficient mice (The Jackson Laboratory, Bar Harbor, ME), backcrossed to C57BL/6 background ≥9 times, were crossbred to obtain four genotypes on an $apoE^{-/-}$ background (abbreviated designations in parentheses): 12/15-$LO^{+/+}$ 5-$LO^{+/+}$ (12+5+; also referred to as "wild type" (wt)), 12/15-$LO^{+/+}$ 5-$LO^{-/-}$ (12+5−), 12/15-$LO^{-/-}$ 5-$LO^{+/+}$ (12−5+), and 12/15-$LO^{-/-}$ 5-$LO^{-/-}$ (12−5−). In addition, $apoE^{+/+}$ (C57BL/6) control mice were used in some experiments. Mice were housed in the Queen's University transgenic animal facility at constant temperature (20–22 °C) and given free access to water and normal chow diet. Experimental mice were housed for 6 months ± 2 weeks of age or until cutaneous xanthomas/dermatitis appeared that are commonly observed in C57BL/6 apoE-deficient mice (25). Tail clip DNA of mice from all colonies was regularly genotyped by PCR after weaning and again after euthanization. For most experiments, mice were weighed and sacrificed by CO_2 inhalation followed by peritoneal lavage (see below). For lipid analysis, blood was collected from the inferior vena cava and allowed to coagulate at room temperature. Following overnight storage at 4 °C, serum was obtained by centrifugation at 2000 × *g* for 5 min and kept at −80 °C until collective analysis for triglycerides (TGs), cholesterol, high density lipoprotein (HDL) and LDL was performed in the Core Laboratory at Kingston General Hospital (Kingston, Ontario, Canada). Spleens were dissected, weighed directly after blood collection, and used to calculate the spleen/body weight ratio (SBR). All experiments were performed in accordance with the guidelines of the Queen's University Animal Care Committee.

Cells—Resident peritoneal exudates were collected from mice immediately after euthanization by peritoneal lavage with 3 × 5 ml of complete medium consisting of RPMI 1640 medium (Sigma) supplemented with 10% fetal bovine serum (HyClone, Fisher Scientific), L-glutamine (HyClone), penicillin, and streptomycin (both from Invitrogen) and kept on ice. Some mice received 1 ml of sterile thioglycollate (TGL) solution (4% in H_2O; Sigma) intraperitoneally 3–4 days prior to euthanization. The exudates were centrifuged (240 × *g* for 10 min at 4 °C), resuspended in complete medium, counted, and plated according to our experimental design. Typically after 1.5–2 h at 37 °C in a 95% air, 5% CO_2 incubator, adhered resident (res-) or TGL-elicited PMΦ were washed twice with phosphate-buffered saline (PBS) to remove non-adherent cells prior to experimentation.

Flow Cytometry—Peritoneal exudate cells were resuspended in PBS containing 5% fetal bovine serum and incubated with 2 μg/ml fluorochrome-tagged primary antibodies for 60 min on ice: anti-CD11b (clone A95-1; BD Biosciences), anti-F4/80 (BM8; Biolegend, San Diego, CA), anti-B220 (RA3-6B2; Biolegend), and respective isotype controls. Cells were washed with PBS plus 5% fetal bovine serum, resuspended in PBS, and kept on ice until analyzed by flow cytometry (FC500, Beckman Coulter, Mississauga, Ontario, Canada). Importantly to prevent artifactual results due to increasing adherence or death of MΦ during sample processing, samples were prepared in random order in each experiment. Propidium iodide staining (1 μg/ml) was used to gate live cells prior to antigen analysis. A total of 50,000 events was recorded per sample. Data were analyzed using CXP analysis software (Beckman Coulter).

RNA Extraction and Real Time PCR Analysis—mRNA was extracted from res- or TGL-elicited PMΦ (TGL-PMΦ) (cultured for 1.5 or 24 h as indicated) using the Qiagen minikit (Qiagen, Mississauga, Ontario, Canada), eluted with 30 μl of DNase-free water, and quantified spectrophotometrically by NanoDrop (Thermo Scientific, Wilmington, DE). Up to 5 μg of RNA were reverse transcribed into cDNA using a SuperScript III Reverse Transcriptase kit (Invitrogen). 50–200 ng of cDNA/well was subjected to real time PCR using the SYBR Green (Applied Biosystems) relative quantification method on an Applied Biosystems 7500 Real Time PCR instrument. Intron-spanning primers were designed to yield amplicons of ~100-bp length for 12/15-LO (forward (f) 5′-GGGCAACTCTTGCCTATAGCC-3′, reverse (r) 5′-AAGTCTGAGCTTCGGACCCA-3′), 5-LO (f 5′-CGGGAACAGCTTATCTGCGA-3′, r 5′-GTCAGATCCTGGACAGCCCTC-3′), 18 S rRNA (f 5′-TGTCTCAAAGATTAAGCCATGCAT-3′, r 5′-AACCATAACTGATTTAATGAGCCATTC-3′), and glyceraldehyde-3-phosphate dehydrogenase (f 5′-CTGGAGAAACCTGCCAAGTA-3′, r 5′-TGTTGCTGTAGCCGTATTCA-3′) with 18 S rRNA or glyceraldehyde-3-phosphate dehydrogenase used as normalizers. Dissociation curve analysis following each amplification reaction was done to confirm specificity of the amplification. RNA expression was determined based on the ΔΔCt comparative method of relative quantification according to the manufacturer. Non-reverse transcribed RNA from wt PMΦ was used as a control to determine contamination by genomic DNA.

Immunocytochemistry—Res-PMΦ were plated on 8-well glass slides (BD Biosciences), washed, fixed using 4% paraformaldehyde, and permeabilized (0.1% Triton X-100 for 10 min). Alternatively peritoneal exudates in complete medium were cytospun (550 rpm for 4 min) onto Superfrost glass slides (Fisher Scientific) either directly or after incubation with 0.44 mM additional $CaCl_2$ and 5 μM ionophore A23187 (Sigma) for 5 min at 37 °C and subsequently fixed in acetone/methanol (1:1) for 5 min at −20 °C. Cells were blocked in 5% normal goat serum (Cedarlane Laboratories, Burlington, Ontario, Canada) in PBS, and primary antibodies in 5% normal goat serum/PBS against murine 12/15-LO (26), 5-LO (LO32; a gift from Dr. J. F. Evans while at Merck Frosst Canada), and/or CD68 (AbD Serotec, Oxford, UK) were applied overnight at 4 °C. The wells were then washed three times; incubated with fluorescein isothiocyanate-coupled goat anti-rabbit antibody and/or Texas Red-coupled goat anti-rat antibody in 5% normal goat serum/PBS (both from Jackson ImmunoResearch Laboratories, West Grove, PA) for 2 h at room temperature; washed three more times; and mounted in Pro-Long Antifade GOLD (Invitrogen) containing 4′,6-diamidino-2-phenylindole. Cytospin slides received an additional blocking step with 5% normal goat serum/PBS between primary and secondary antibody application. Fluorescence micrographs were acquired with a Zeiss fluorescence microscope using 40× or 100× oil immersion objectives.

Western Blotting—Res-PMΦ were lysed by sonication in T-PER reagent (Pierce) supplemented with a protease inhibitor mixture (Roche Applied Science) and centrifuged (13,000 × *g* for 5 min). Aliquots of the supernatant were mixed with 2× Laemmli buffer and subjected to SDS-PAGE in 10% gels using a Bio-Rad Mini Protean system. After blotting to Immobilon-P membranes (Millipore, Etobicoke, Ontario, Canada) and blocking in 2% dry milk, Tris-buffered saline, primary antibodies (in 5% bovine serum albumin, Tris-buffered saline) against murine 12/15-LO (26), 5-LO (LO32), or β-actin (Sigma) were applied overnight at 4 °C followed by secondary antibodies (Sigma) and detection using an ECL chemiluminescence kit (GE Healthcare).

Eicosanoid Analysis—Res-PMΦ from three to four mice were pooled and plated in two wells of a 6-well plate (Corning, Lowell, MA) in complete medium, washed after 1.5 h, and supplemented with 1.8 ml of colorless Dulbecco's modified Eagle's medium (D1145, Sigma) containing penicillin/streptomycin but no fetal bovine serum. Cells ($(3.0 \pm 0.5) \times 10^6$/well) were primed with phorbol myristate acetate (75 nM; Sigma) for 45 min and preincubated with COX-1 inhibitor SC-560 (10 μM; Cayman Chemical (27)) or vehicle for 20 min. Then eicosanoid biosynthesis from endogenous AA was induced by an additional 0.44 mM $CaCl_2$ and 5 μM ionophore A23187 (Sigma). After 45 min, 200 μl of ethanol was added, and the medium was collected immediately. The total cellular protein of each sample was established by T-PER extraction and the Bradford method (Bio-Rad). To the medium, prostaglandin (PG) B_2 (50 ng; Cayman Chemical) as internal standard and 1 N HCl (20 μl) for acidification were added followed by centrifugation (2000 × *g* for 10 min) and purification using Alltech C_{18} solid-phase extraction columns (Fisher Scientific). The eluate in methanol was evaporated to dryness, resuspended in 80 μl of methanol, centrifuged (16,000 × *g* for 10 min), and filtered through 0.22-μm particle filters (Waters). Aliquots (5 μl) were injected on a Waters Acquity C_{18} column (2.1 mm × 100 mm, 1.7-μm particle size) in a Waters Acquity Ultra-Performance Liquid Chromatography (UPLC) system. HETEs and leukotrienes were eluted isocratically with a mixture of acetonitrile, methanol, water, and acetic acid (45:24:31:0.007) and detected at 235 nm (HETEs) or 278 nm (PGB_2, LTB_4 and LTB_4 isomers) by a photodiode array detector. The remainder of the samples was used for liquid chromatography-tandem mass spectrometry (LC-MS/MS) analysis. Each sample was injected into an high pressure liquid chromatography gradient pump system directly interfaced to the electrospray source of a Sciex API 3000 triple quadrupole mass spectrometer (PE Sciex, Toronto, Canada) equipped with a Gemini 5-μm C_{18} (2.0 × 150-mm) column (Phenomenex, Torrance, CA). Starting from 55% solvent A (water/acetic acid, pH 5.7; v/v), 45% solvent B (acetonitrile/methanol, 65:35, v/v), analytes were eluted on a linear gradient up to 80% solvent B followed by an increase to 98% solvent B and isocratic elution at 98% solvent B. Eicosanoids were detected in the negative ion mode by multiple reaction monitoring of *m*/*z* 369 → 169 for thromboxane (Tx) B_2, *m*/*z* 351 → 271 for PGE_2, *m*/*z* 333 → 235 for PGB_2, *m*/*z* 624 → 272 for LTC_4, *m*/*z* 335 → 195 for LTB_4 and the 6-*trans*-LTB_4 isomers, *m*/*z* 335 → 115 for 5,6-diHETE, *m*/*z* 335 → 201 for 5,15-diHETE, *m*/*z* 351 → 115 for both lipoxin A_4 and lipoxin B_4, *m*/*z* 319 → 115 for 5-HETE, *m*/*z* 319 → 155 for 8-HETE, *m*/*z* 319 → 151 for 9-HETE, *m*/*z* 319 → 167 for 11-HETE, *m*/*z* 319 → 179 for 12-HETE, *m*/*z* 319 → 219 for 15-HETE, and *m*/*z* 303 → 205 for AA. Although neither lipoxin A_4 nor lipoxin B_4 could be detected in these studies, the limit of detection of our method was determined to be 50–100 pg injected on column. Eicosanoids were quantified using PGB_2 as an internal standard with standard curves calculated for PGE_2, TxB_2, LTC_4, LTB_4, 5-HETE, and AA. The LTB_4 curve was also used to quantify the 6-*trans*-LTB_4 isomers, 5,6-diHETE, and 5,15-diHETE. The 5-HETE curve was used to quantify 8-HETE, 9-HETE, 11-HETE, 12-HETE, and 15-HETE. Each of the standard curve points was solid-phase-extracted to account for differences in recovery as compared with PGB_2. Presented data were calculated from initial area analyte/area PGB_2 data, normalized to protein content, and converted to ng of analyte/mg of protein.

In Vivo Peritonitis Model—Mice (8–14 weeks) were anesthetized with ketamine/xylazine and placed on a heated pad. Evans Blue dye (0.5% aqueous solution in saline; General Diagnostics, Warner Chilcott) was injected into the tail vein as a weight-corrected volume (200 μl/25 g of body weight) followed by an intraperitoneal injection (500 μl) of zymosan (stock 2 mg/ml in PBS, boiled and washed; Sigma) or PBS. After 60 min, mice were killed by cervical dislocation, and the peritoneal exudate was collected using 3 ml of PBS. Exudates were centrifuged (240 × *g*), and supernatants were analyzed for Evans Blue bound to plasma albumin at 595 nm in a plate reader (Fluostar Optima, BMG Labtech, Fisher Scientific) and for eicosanoid levels as mentioned above.

Lipoprotein Uptake Assay—LDL was isolated from EDTA-anticoagulated blood (25 ml) drawn from healthy volunteers

(approved by Queen's University Health Sciences Research Ethics Board) by sequential ultracentrifugation (28) with modifications. In brief, plasma was adjusted with NaBr (Sigma) to a density of 1.02 g/ml and centrifuged at 100,000 × *g* for 2 h at 4 °C, and the infranatant was collected. Phenylmethanesulfonyl fluoride (1 mM; Sigma) was routinely added to prevent proteolysis. The lipoprotein solution was then adjusted to a density of 1.063 g/ml with NaBr and centrifuged again under the conditions described above. The LDL-containing supernatant was collected and dialyzed twice in Slide-A-Lyzer cassettes (cutoff, 2,000 kDa; Pierce) against 20 mM HEPES and 150 mM NaCl, pH 7.4 for 4 and 18 h followed by protein assay according to the Bradford method. Native (n) LDL (approximately 1 mg/ml) was stored under nitrogen gas at 4 °C in the dark. Acetylated (Ac) LDL was obtained by mixing 200 μl of nLDL with 200 μl of saturated sodium acetate solution and 5 additions of 1 μl pure acetic anhydride (Sigma) in 10 min intervals during continuous rotation at 4 °C based on (29). After additional rotation for 30 min, the solution was dialyzed as described above against 150 mM NaCl, 400 μM EDTA, pH 7.4 for 4 and 18 h. Aliquots of nLDL and AcLDL were assessed for protein content by the Bradford test and analyzed for successful modifications on a 0.5% agarose gel in barbital buffer (Sigma). Purity and integrity of the preparations were assured using a 4–20% Tris-glycine gradient gel (Invitrogen) followed by silver staining.

Res-PMΦ were maintained in 8-well slides for 1.5 h after extraction, washed twice with PBS, and exposed to nLDL (100 μg/ml) or AcLDL (40 μg/ml) dissolved in minimal medium for 24 h at 37 °C and 5% CO_2. Following careful washing (three times) with PBS, cells were fixed in 10% buffered formalin (Fisher Scientific) for 30 min, washed briefly, and stained for lipids by Oil Red O (Sigma). Counterstaining was done using Harris' modified hematoxylin (Fisher Scientific). Cells were mounted in AquaPerm (Shandon Immunon, Fisher Scientific), allowed to dry overnight, and mounted in Cytoseal 280 (Fisher Scientific) plus a coverslip prior to analysis by bright field microscopy (40×; Zeiss). Res-PMΦ with ≥1 lipid droplet were defined as positive, and the number of medium sized lipid droplets (diameter, 1–2 μm) was counted and averaged per positive cell.

Aortic Root and en Face Lesion Analysis—Mice were kept on regular chow diet until 6 months ± 2 weeks of age and then euthanized. After peritoneal lavage and blood collection from the inferior vena cava, vessels were perfused with copious amounts of ice-cold PBS through the left ventricle. Aortae were dissected from the heart to the iliac bifurcation and fixed in 10% buffered formalin (Fisher Scientific) overnight. Hearts with aortic roots were embedded in Tissue-Tek optimal cutting temperature compound. (VWR International, Mississauga, Ontario, Canada) and frozen at −80 °C until 8-μm sections were cut with a Cryostat (Leica, Richmond Hill, Ontario, Canada). Sections were washed with water for 10 min, fixed in 10% buffered formalin, and stained with Oil Red O and hematoxylin. Analysis of micrographs taken with a 5× objective was performed using Image-Pro Plus software (Media Cybernetics, Silver Spring, MD). The total lesion area of three to four sections per mouse was averaged. Fixed entire aortae were washed in PBS, cleaned, opened longitudinally, stained with Sudan IV (Sigma), and pinned on wax (Minutien Insect Pins, Fine Science Tools, North Vancouver, British Columbia, Canada). En face lesion area relative to the total aortic area was determined using Image-Pro Plus software.

Statistics—Data are expressed as mean ± S.E. Statistical analysis (one-way analysis of variance or Student's *t* test for unpaired or paired observations as appropriate or Fisher's exact test for non-parametric analysis) was performed using GraphPad InStat software (La Jolla, CA). A p value of <0.05 (*) was considered significant (**, $p < 0.01$).

RESULTS

Comparative Analysis of Lipoxygenase Transcripts Reveals Significant Differences between Macrophage Populations—Inhibition of either 12/15-LO or 5-LO enzymes has been considered as potential therapy for cardiovascular disease (3, 24, 26). To examine the effects of inhibition of both enzymes simultaneously, we generated dual 12/15-LO- and 5-LO-deficient mice on an atherosclerosis-susceptible apoE-deficient background and characterized LO-expressing macrophages. TGL-PMΦ are a frequently used source of macrophages. However, these cells show phenotypic disparities compared with res-PMΦ (30). We sought to compare relative transcript levels of 12/15-LO and 5-LO in TGL-PMΦ and res-PMΦ and to verify the knock-out status of the four strains of mice. Strikingly wt TGL-PMΦ cultured 1.5 h *ex vivo* expressed only 1% of the quantity of 12/15-LO transcripts detected in res-PMΦ from wt mice (Fig. 1*A*). TGL-PMΦ from the other three genotypes, including 12/15-LO$^{-/-}$ cells, showed similar low expression presumably due to residual transcriptional activity of the 12/15-LO neomycin cassette-disrupted allele. Likewise 12−5− res-PMΦ displayed 3.5% residual expression compared with wt (Fig. 1*A*). However, transcripts with gene-disrupting neomycin cassettes (confirmed by genotyping) do not translate a functional enzyme (12, 18). 5-LO mRNA transcripts in TGL-PMΦ from wt mice were detected at only 28% the level found in wt res-PMΦ and were virtually undetectable in 5-LO$^{-/-}$ cells, thus verifying the knock-out (Fig. 1*B*). We also investigated 12/15-LO and 5-LO transcripts in res-PMΦ cultured *ex vivo* for 24 h. Notably the relative quantities of 12/15-LO and 5-LO transcripts were reduced to 42 ± 7 and 52 ± 9%, respectively, of the levels found in macrophages cultured for 1.5 h. These results established that only wt res-PMΦ, but not TGL-PMΦ, cultured for 1.5 h show a high abundance of 12/15-LO and 5-LO mRNA transcripts and are the most suitable cells and conditions to study LO-dependent effects.

Assessment of Lipoxygenase Protein Levels in Macrophages—We verified the phenotypic knock-out of both LO proteins in res-PMΦ by immunofluorescence microscopy. Whereas wt cells (Fig. 2, *A*, *B*, *E*, and *F*) displayed strong immunostaining for 12/15-LO (Fig. 2, *A* and *B*) and 5-LO (Fig. 2, *E* and *F*), 12−5− cells (cultured for 2 h) were negative (Fig. 2, *C*, *D*, *G*, and *H*). 12/15-LO and 5-LO were also detected by Western blotting in res-PMΦ from wt mice but not from 12–5- mice (Fig. 2*I*). To visualize the subcellular localization of both LOs, resting wt cells were cultured for 18 h to allow for acquisition of characteristically spread morphology. Clearly 12/15-LO localized to the cytoplasm (Fig. 2, *A* and *B*), whereas 5-LO was detected

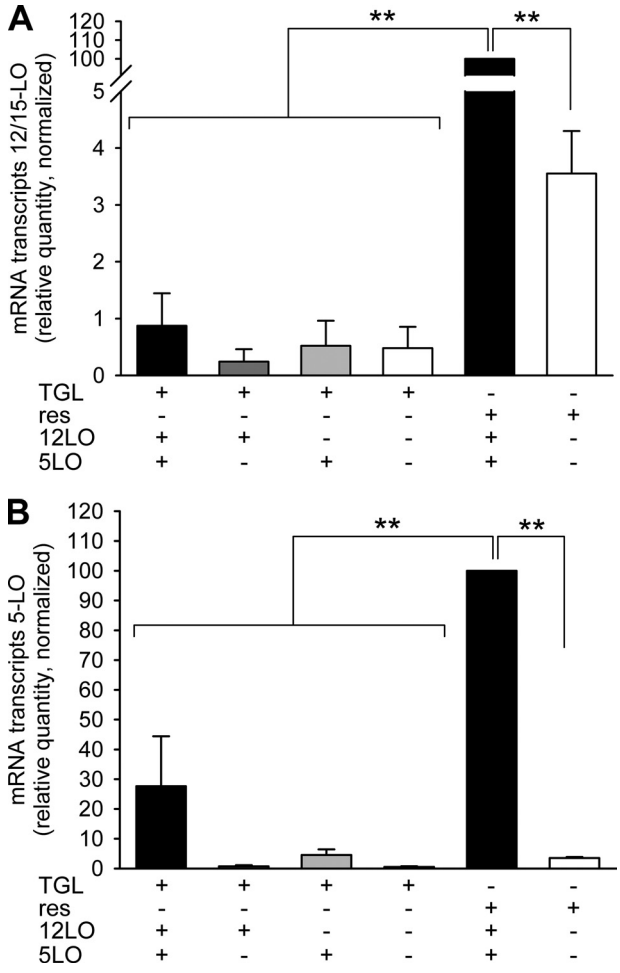

FIGURE 1. **Analysis of 12/15-LO and 5-LO mRNA transcripts in peritoneal macrophages.** mRNA levels of 12/15-LO and 5-LO were investigated in resident or TGL-elicited PMΦ cultured 1.5 h *ex vivo*. The figure shows relative quantities of 12/15-LO (*A*) or 5-LO (*B*) mRNA transcripts in TGL-PMΦ (*TGL*) or res-PMΦ (*res*) from LO-positive (+) or -negative (−) cells normalized to res-PMΦ from wt mice (set to 100). Data are expressed as mean ± S.E. of $n = 2–6$ independent experiments and were analyzed by analysis of variance. **, $p < 0.01$.

within the nucleus (Fig. 2, *E* and *F*). We determined whether this distribution is also found in freshly extracted cells from the peritoneal cavity. No major difference was apparent for 12/15-LO. However, 5-LO was evenly dispersed in the cytoplasm and in the nucleus with some accumulation at the nuclear envelope (supplemental Fig. 1, A and C). Brief (5-min) stimulation by Ca^{2+} ionophore A23187, a strong cellular stimulus applied in the eicosanoid biosynthesis experiments (see below), caused 5-LO to become enriched (punctate staining) inside the nucleus and at the nuclear envelope, whereas 12/15-LO displayed only a slight redistribution to cytoplasmic and nuclear membranes (supplemental Fig. 1, B and D).

Altered Eicosanoid Profiles in LO-deficient Res-PMΦ—As MΦ play important roles in atherosclerosis, inflammation, and immunity (31), they produce a variety of inflammatory lipid mediators. We assessed the eicosanoid profiles of res-PMΦ in relation to the presence or absence of 12/15-LO and 5-LO. In addition, we analyzed the effects of pharmacological COX-1 inhibition by SC-560 (27). Priming by phorbol myristate acetate and stimulation by Ca^{2+} ionophore induced endogenous AA

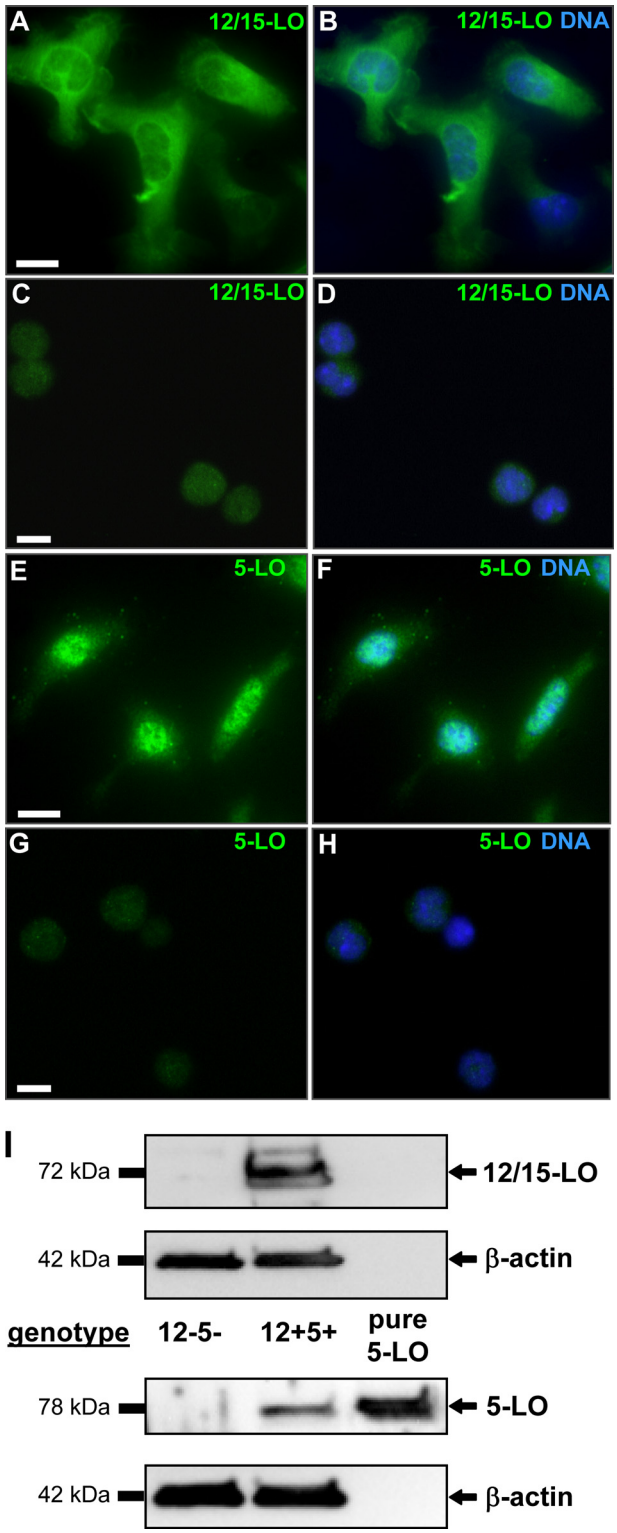

FIGURE 2. **Lipoxygenase expression in resident peritoneal macrophages.** Res-PMΦ were seeded on 8-well glass slides, fixed, and immunolabeled for LOs. Cells from wt mice (*A*, *B*, *E*, and *F*) were cultured for 18 h to allow cell spreading, which revealed mostly cytoplasmically localized 12/15-LO (*A* and *B*) and nuclear 5-LO (*E* and *F*). Cells from 12−5− mice (*C*, *D*, *G*, and *H*) displayed only background fluorescence for 12/15-LO (*C* and *D*) and 5-LO (*G* and *H*). Overlays with nuclear 4′,6-diamidino-2-phenylindole staining (*B*, *D*, *F*, and *H*) show co-localization with 5-LO (*F*) but not with 12/15-LO (*B*) in 12+5+ cells. *Scale bar*, 10 μm. *I*, Western blot detection of proteins (12/15-LO, 5-LO, and β-actin) in lysed res-PMΦ. Purified 5-LO protein (*lane 3*) was used as positive control. Blots and micrographs are representative of at least three independent experiments.

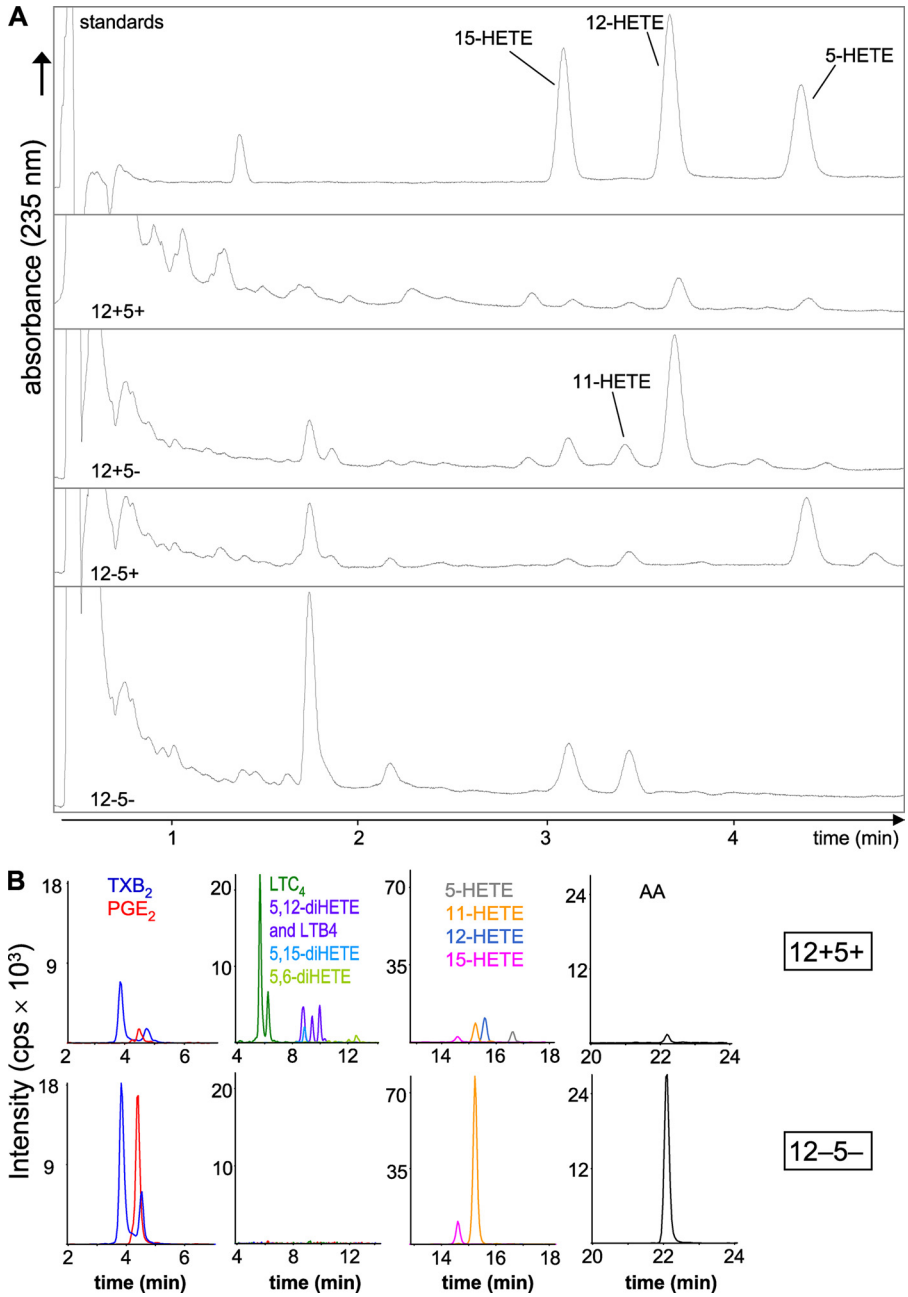

FIGURE 3. **Eicosanoid detection in resident peritoneal macrophage incubations.** Pooled res-PMΦ from three to four mice were primed with phorbol myristate acetate and preincubated with or without the COX-1 inhibitor SC-560 for 20 min. Eicosanoid biosynthesis from endogenous AA was activated by 0.44 mM additional $CaCl_2$ and 5 μM ionophore A23187 and analyzed after 45 min. *A*, representative UPLC chromatograms of HETEs detected at 235 nm from all four genotypes and the internal standard mixture (*top* trace) are shown ($n \geq 3$). *B*, representative LC-MS/MS chromatograms of a 12+5+ sample (*top row*) and a 12−5− sample (*bottom row*) were graphically separated to improve clarity. The 12−5− sample shown had a higher analyte recovery, reflected by the PGB_2 internal standard peak area (not shown). *cps*, counts/s.

release, LO activation, and partial translocation (supplemental Fig. 1, B and D). The presence or absence of the 12/15-LO products 12-HETE and 15-HETE and the 5-LO product 5-HETE displayed in UPLC chromatograms recorded at 235 nm verified the functional knock-out of 12/15-LO and/or 5-LO in the respective genotypes (Fig. 3*A*). Surprisingly 15-HETE was detected in 12−5− cells along with increased amounts of 11-HETE (Fig. 3*A*). This prompted us to investigate the levels of several important eicosanoids and free AA in more detail using LC-MS/MS normalized to cellular protein content (Figs. 3*B* and 4).

As evident in Fig. 4*A*, absence/inhibition of both LOs or of 12/15-LO and COX-1 increased the quantity of free AA drastically, peaking in a 90-fold rise with dual LO deficiency and COX-1 inhibition. The COX products PGE_2 and TxA_2 (detected as stable metabolite TxB_2) were inhibited, albeit incompletely (60–90%), upon incubation with 10 μM SC-560. Interestingly COX products were not or were only moderately increased in all LO knock-out samples (Fig. 4, *B* and *C*). Based on the effects of SC-560, 11-HETE is a predominant COX-1 product, whereas 12-HETE is solely generated by 12/15-LO (Fig. 4, *G* and *H*), thus confirming our initial UPLC observations (Fig. 3*A*). In contrast, although 15-HETE is formed primarily by 12/15-LO in cells of 12/15-LO^+ genotype, genetic inactivation of 12/15-LO revealed that substantial quantities of 15-HETE can be formed by COX-1 especially when 5-LO was inactivated in parallel (Fig. 4*I*). A participation of COX-1 in 15-HETE synthesis might explain why in wt cells 15-HETE increased 2.8-fold upon COX-1 inhibition, whereas the COX-independent product 12-HETE increased 5.2-fold upon COX-1 blockage (Fig. 4, *H* and *I*). 8-HETE and 9-HETE were minor products detected (not shown). All detectable diHETEs, including LTB_4 for comparison, are summarized in Fig. 4*J*. 5,6-diHETE and LTB_4 were dependent entirely on 5-LO and correlated to the amounts of 5-HETE (Fig. 4*D*). LTB_4 isomers as well as several other 5,12-diHETE isomers, surprisingly, were also detected in 12+5− cells especially with concomitant COX-1 inhibition. 5,15-diHETE was only synthesized in wt cells (Fig. 4*J*). 8,15-diHETE as well as the triHETEs lipoxin A_4 and B_4 were not present in detectable quantities. Taken together, substantial shifts in the abundance and utilization of free AA occur in res-PMΦ depending on the presence of functional COX-1 and LO metabolic pathways, revealing appreciable substrate diversion into LO pathways when COX-1 is blocked.

Spleen Weight and Peritoneal Lavage Cell Assessment—12/15-LO was suggested to be involved in myeloproliferative dis-

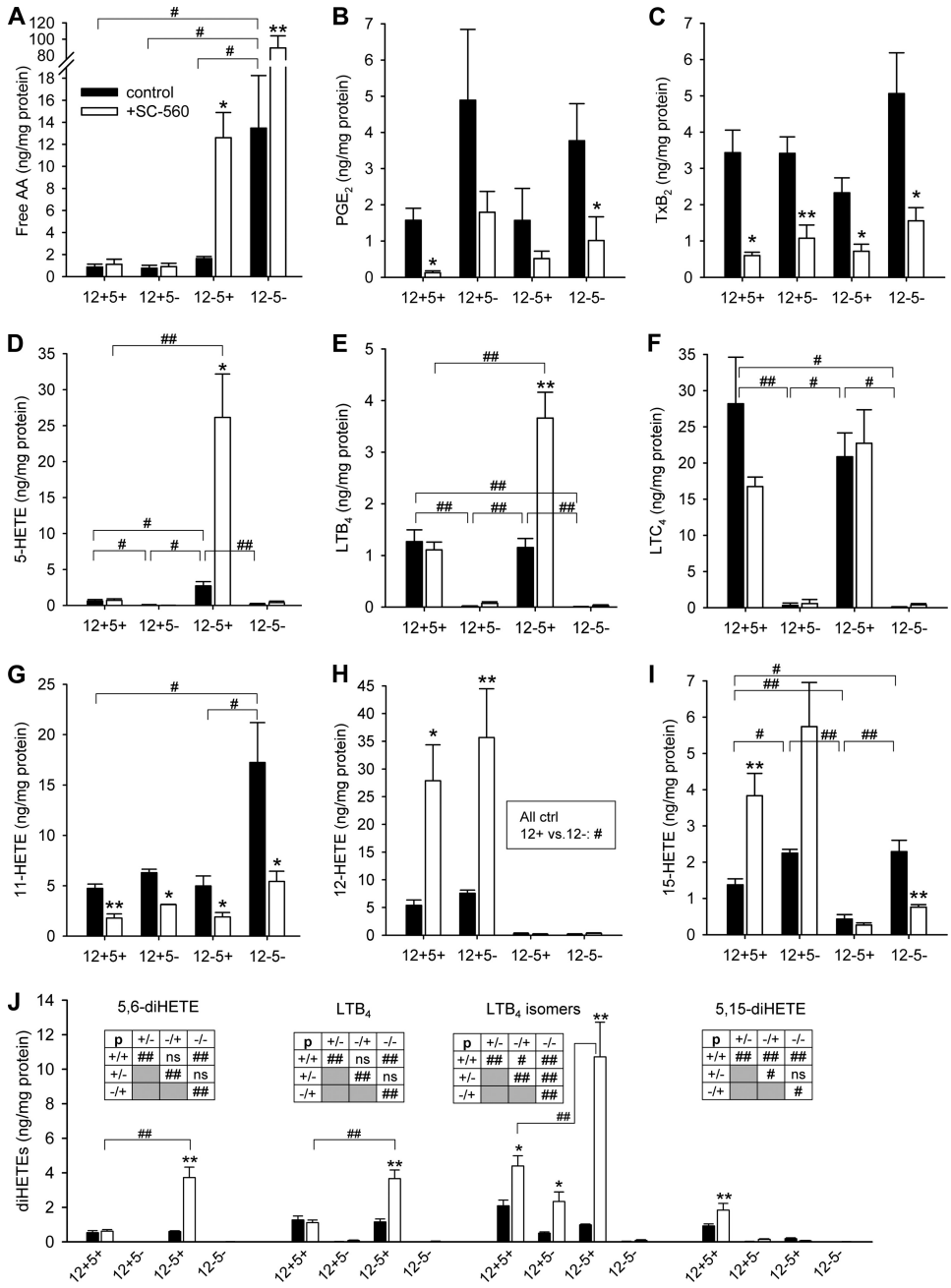

FIGURE 4. **Altered eicosanoid profiles of resident peritoneal macrophages with LO deficiency and COX-1 inhibition (SC-560).** Samples were prepared as described for Fig. 3 and analyzed by LC-MS/MS. Figures show paired data of control (*black bars*) and SC-560-treated cells (*open bars*) of all four genotypes, including free AA (*A*), PGE_2 (*B*), TxB_2 (*C*), 5-HETE (*D*), LTB_4 (*E*), LTC_4 (*F*), 11-HETE (*G*), 12-HETE (*H*), 15-HETE (*I*), and 5,6-diHETE, LTB_4, 5,12-diHETE isomers, and 5,15-diHETE (all *J*). Data are expressed as mean ± S.E. from two to five independent experiments determined over two LC-MS/MS runs. Statistical comparisons between paired bars (±SC-560) are indicated with * ($p < 0.05$) or ** ($p < 0.01$). All significant differences are shown. Comparisons between genotypes are labeled with # ($p < 0.05$) or ## ($p < 0.01$). In *J*, statistics of comparisons between *black bars* are presented in *boxed insets*. *ctrl*, control; *ns*, not significant.

orders as indicated by increased spleen weights (32). Average spleen weights in our mice at the time of euthanization (≤6 months) were 108 ± 4 (12+5+), 115 ± 6 (12+5−), 124 ± 7 (12−5+), and 126 ± 4 mg (12−5−). Female mice displayed higher SBRs than their male counterparts (Fig. 5*A*), and mice lacking 12/15-LO consistently showed increased SBRs compared with wt mice (Fig. 5*A*, *box*). In addition, 12−5− mice had larger spleens than 12−5+ mice. However, occasional drastic increases in spleen weights as reported previously (32) were not observed. Mice lacking 12/15-LO or both LOs tended to have lower body weights (Fig. 5*B*). Up to 6 months, the maximum time point studied, our mice frequently developed cutaneous xanthomas/dermatitis (Fig. 5*C*) as previously reported for apoE-deficient mice (25).

We assessed a potential impact of genetic LO deletions on myeloid populations in peritoneal lavages. A reduced percentage of mature $CD11b^+$ $F4/80^+$ MΦ (supplemental Fig. 2, A and C) and $B220^+$ B lymphocytes (supplemental Fig. 2, B and D) was detected in peritoneal lavages of 12/15-LO-null mice as compared with wt mice. This reduction was, however, not apparent in dual LO-deficient mice where $B220^+$ cells were even increased (supplemental Fig. 2).

5-LO or Dual LO Deficiency Attenuates Peritonitis—Intraperitoneal injection of zymosan activates local inflammatory cells and results in increased plasma leakage into the peritoneal cavity (33). We assessed the requirement of LOs for this process in zymosan-induced peritonitis. Plasma protein leakage induced by zymosan injection was enhanced 3-fold in wt cells and 2.5-fold in 12−5+ mice (Fig. 6*A*). Significantly reduced leakage was evident in 12+5− and 12−5− mice (1.9- and 1.7-fold, respectively, above PBS control). This likely resulted from the complete absence of the major 5-LO products (cysteinyl leukotrienes) in these two groups of mice (Fig. 6*B*) indicating a role for 5-LO in regulating vascular permeability. Prostaglandins, LTB_4, and diHETEs were not detectable under our assay conditions. PBS-injected animals used as controls displayed similar background leakage between all genotypes (absorbance readings of 0.089–0.19), and 12-HETE and 15-HETE were the only detectable eicosanoids under these basal conditions (Fig. 6*B*).

Serum Lipid Levels—As a prerequisite to our atherosclerosis study (below), we analyzed serum lipid levels in apoE-deficient mice with different LO genotypes. Compared with wt mice, lack of one or both LOs did not appreciably affect serum TG and total, HDL, or LDL cholesterol levels in the knock-out geno-

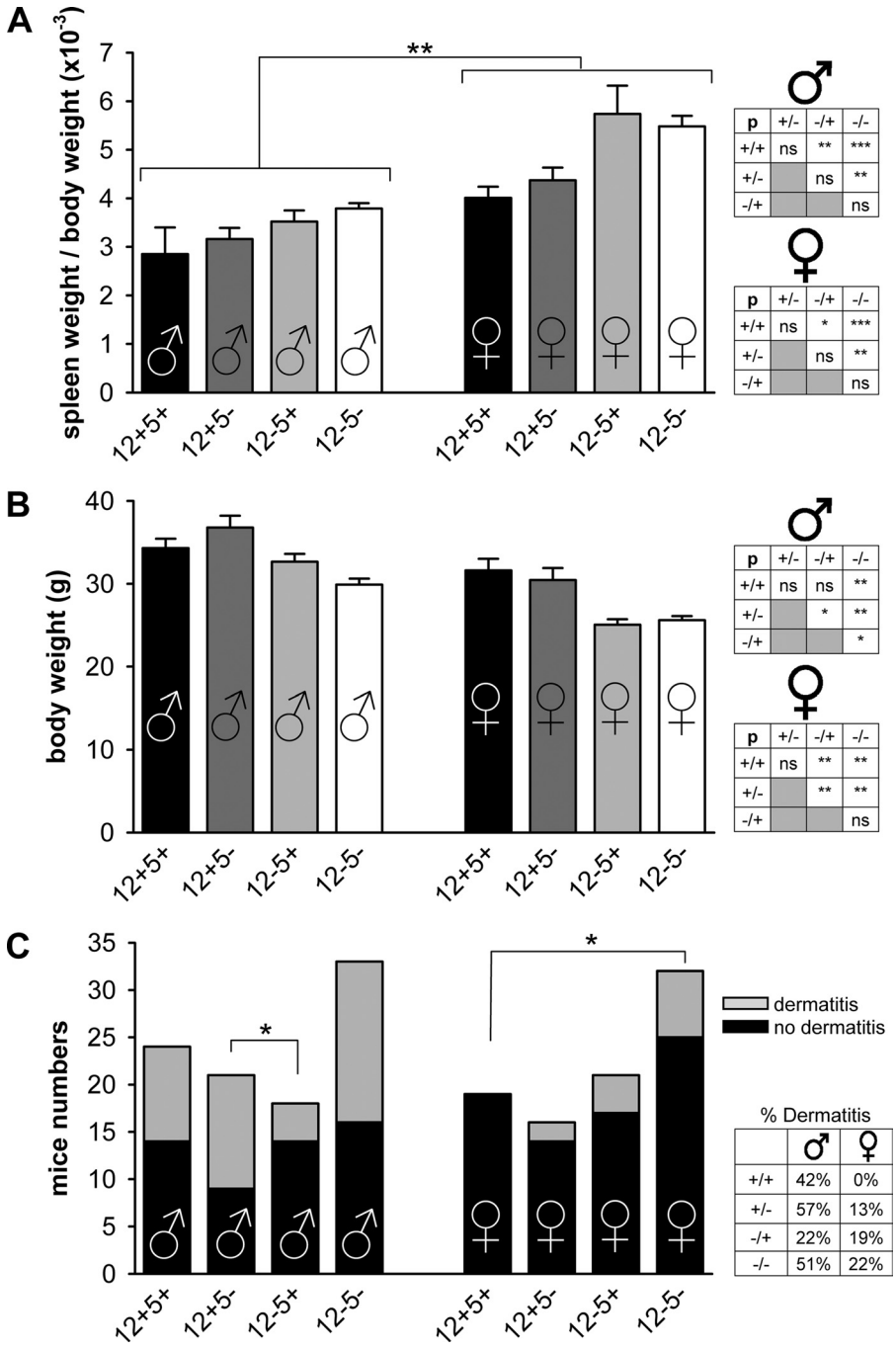

FIGURE 5. **Spleen weight assessment.** The SBR (*A*) and absolute body weights (*B*) of mice (average ages, 20–24 weeks) are shown. Significantly increased SBR was observed in each genotype for the female (♀) (*right*) over the respective male (♂) (*left*) population as well as between certain genotypes within each gender group. Statistical comparisons within each gender are displayed in *inset boxes* to the *right* (*, $p < 0.05$; **, $p < 0.01$; ***, $p < 0.005$; *ns*, not significant). Note that *inset* genotypes are abbreviated (+/+ represents 12+5+; −/− represents 12−5−; mixed genotypes represented accordingly). *C*, occurrence of cutaneous xanthomas/dermatitis in each group, sorted by gender. Relative occurrence (in percent) is displayed in a *box* to the *right*. Data in *C* were compared by Fisher's exact non-parametric test. A total of 43 (+/+), 38 (+/−), 39 (−/+), and 64 (−/−) mice was analyzed.

types (Fig. 7, *A–D*). TG levels were somewhat lower in 12−5− mice (Fig. 7*A*), and both genotypes lacking 12/15-LO showed a trend toward reduced HDL serum concentrations (Fig. 7*C*). Lipid levels were in the expected range for apoE-deficient mice with about 5- and 8-fold increased cholesterol and LDL levels, respectively, and 3-fold raised TG levels as compared with C57BL/6 control mice (not shown) (34). Thus, deficiency of 12/15-LO and/or 5-LO did not significantly modulate physiological serum lipid concentrations in apoE$^{-/-}$ mice used in these studies.

Lipoprotein Uptake—MΦ ingesting modified LDL and turning into foam cells are a hallmark of atherogenesis (19). Multiple studies have indicated roles for 12/15-LO and 5-LO in various aspects of the atherogenesis process (for a review, see Ref. 3). Extending previous work showing an impaired uptake of LDL in PMΦ lacking 12/15-LO (11), we compared the *in vitro* capacity of res-PMΦ to accumulate nLDL and AcLDL in all four genotypes. nLDL uptake was not different between genotypes (Fig. 8*A*). However, mice deficient for both LOs showed diminished AcLDL uptake compared with wt cells (Fig. 8, *B–F*).

Aortic Root and en Face Lesion Analysis—The atherosclerotic burden of 6-month-old healthy mice fed regular chow diet was examined by two experimental approaches. First cross-sections of the aortic root were stained for lipids and cholesterol with Oil Red O. Female mice with both 12/15-LO and 5-LO deficiency displayed a ≈40% reduction in aortic root lesion area with no significant differences between groups of male mice (Fig. 9, *A* and *B*). En face lesion analysis of the entire aorta from the aortic root to the iliac bifurcation revealed significantly reduced lesion areas for female mice of either the 12−5+ (−50%) or 12−5− (−37%) genotypes as compared with wt mice (Fig. 9, *C* and *D*). Male mice had fewer lesions altogether and no differences between genotypes (Fig. 9*C*). These results demonstrate, therefore, that the severity of atherosclerotic lesion development was markedly reduced at the aortic root and throughout the entire aorta of female mice lacking both 12/15-LO and 5-LO.

DISCUSSION

12/15-LO and 5-LO represent the two lipoxygenase family members most studied with respect to inflammation and cardiovascular disease (1–5, 20). Information about the interrela-

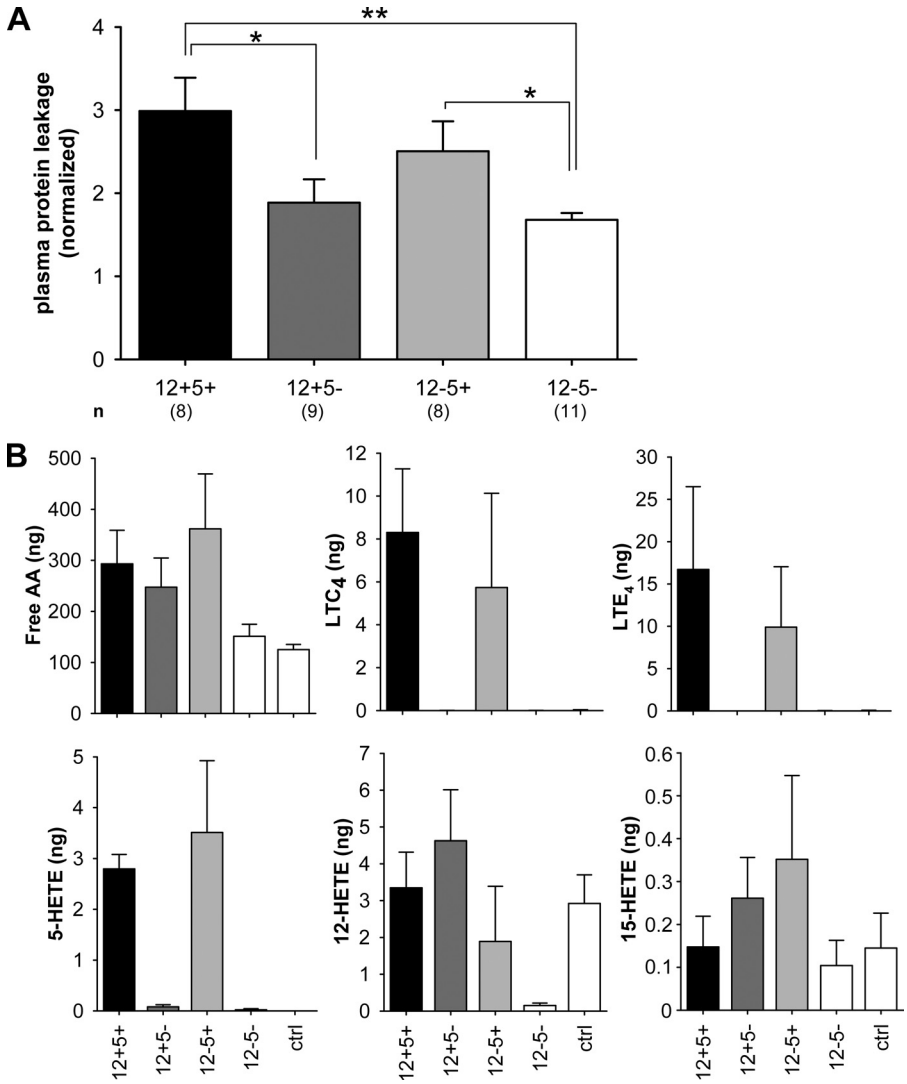

FIGURE 6. **5-LO or dual LO deficiency attenuates zymosan-induced peritonitis.** Anesthetized mice received an intravenous injection of Evans Blue dye followed by an intraperitoneal injection of zymosan to induce peritonitis. *A*, exudates were collected after 60 min and analyzed for Evans Blue leakage spectrophotometrically at 595 nm. Data (mean ± S.E., $n = 8–11$) were normalized to PBS controls (*, $p < 0.05$; **, $p < 0.01$). *B*, levels of free AA and other detected eicosanoids in exudates of zymosan- or PBS (control (*ctrl*))-injected mice. A total of $n = 4–7$ samples was analyzed.

tionship of these two LO enzymes in cellular and pathophysiological contexts is very limited. Therefore, we analyzed the consequences of dual LO inhibition for the first time using a genetic strategy of inactivation of both 12/15-LO and 5-LO on an apoE-deficient background in macrophages, zymosan-induced peritonitis, and atherosclerosis.

12/15-LO and 5-LOs are expressed predominantly in selected cell types of the myeloid lineage (2, 8, 15), and they show differential intracellular localization (cytoplasm *versus* nucleus, respectively; supplemental Fig. 1). Among these, res-PMΦ constitute the one major cell type with abundant expression of both enzymes in mice (Refs. 2, 11, and 12; Figs. 1 and 2; and supplemental Fig. 1). However, their expression decreases with time of culture, a phenomenon documented previously for 12/15-LO in adherent res-PMΦ (35). TGL-elicited PMΦ derive from monocytes recruited from the bloodstream and are phenotypically distinct (30). These cells exhibit minimal expression of 12/15-LO (1% of res-PMΦ levels; Fig. 1 and see also Refs. 16 and 36) and greatly reduced 5-LO levels (28% of res-PMΦ levels; Fig. 1). TGL causes mild peritoneal inflammation (30) and presumably activates resident phagocytes, which attract additional inflammatory monocytes/macrophages, perhaps by means of 5-LO-derived and dual 5-LO-/12/15-LO-derived chemoattractants (*e.g.* LTB_4, 5,12-diHETE, 5,15-diHETE, and 8,15-diHETE isomers) (1, 8, 22), which were detected in macrophage incubations (Fig. 4).

We tested the role of both LO enzymes in a model of inflammatory peritonitis induced by zymosan injection and observed significantly reduced plasma leakage, a measure of endothelial cell activation and vascular permeability, in 5-LO-deficient and dual LO-deficient mice compared with wt (Fig. 6*A*). Decreased plasma leakage was also reported previously for single 5-LO-deficient mice (6) as well as for LTA_4 hydrolase-deficient mice (37), supporting a role for the 5-LO pathway in this model. Cysteinyl LT receptors are prime suspects to mediate the vascular permeability events (7). The onset of peritoneal inflammation, as demonstrated by TGL elicitation of phagocytes (Fig. 1) and by *Staphylococcus epidermidis* supernatants (38), is accompanied by the advent of 12/15-LO-negative cells and the disappearance of 12-HETE from the peritoneal cavity (38). It may, therefore, be hypothesized that products of 12/15-LO are only required under homeostatic "resident" conditions but not during acute inflammation. This is supported by the fact that subcellular relocalization upon acute PMΦ activation did not occur for 12/15-LO (supplemental Fig. 1). In contrast, 5-LO is considered a quiescent enzyme that typically becomes activated when the host cell acquires an inflammatory phenotype as evident by peri- or intranuclear accumulation of 5-LO upon MΦ activation (supplemental Fig. 1 and Ref.13) and LT biosynthesis at the nuclear membrane (14). Interestingly lack of 12/15-LO products caused a relative reduction of MΦ and $B220^+$ B cells in the peritoneal cavity (supplemental Fig. 2), apparently perturbing an equilibrium of antagonistic 12/15-LO and 5-LO products on myeloid cell migration under homeostatic conditions. Concomitant deletion of 5-LO restored the balance of normal MΦ percentages in the cavity (supplemental Fig. 2). Exactly how 5-LO-derived metabolites might synergize with 12/15-LO products to orchestrate inflammatory events and the subsequent proresolving aspects (10, 39) remains to be

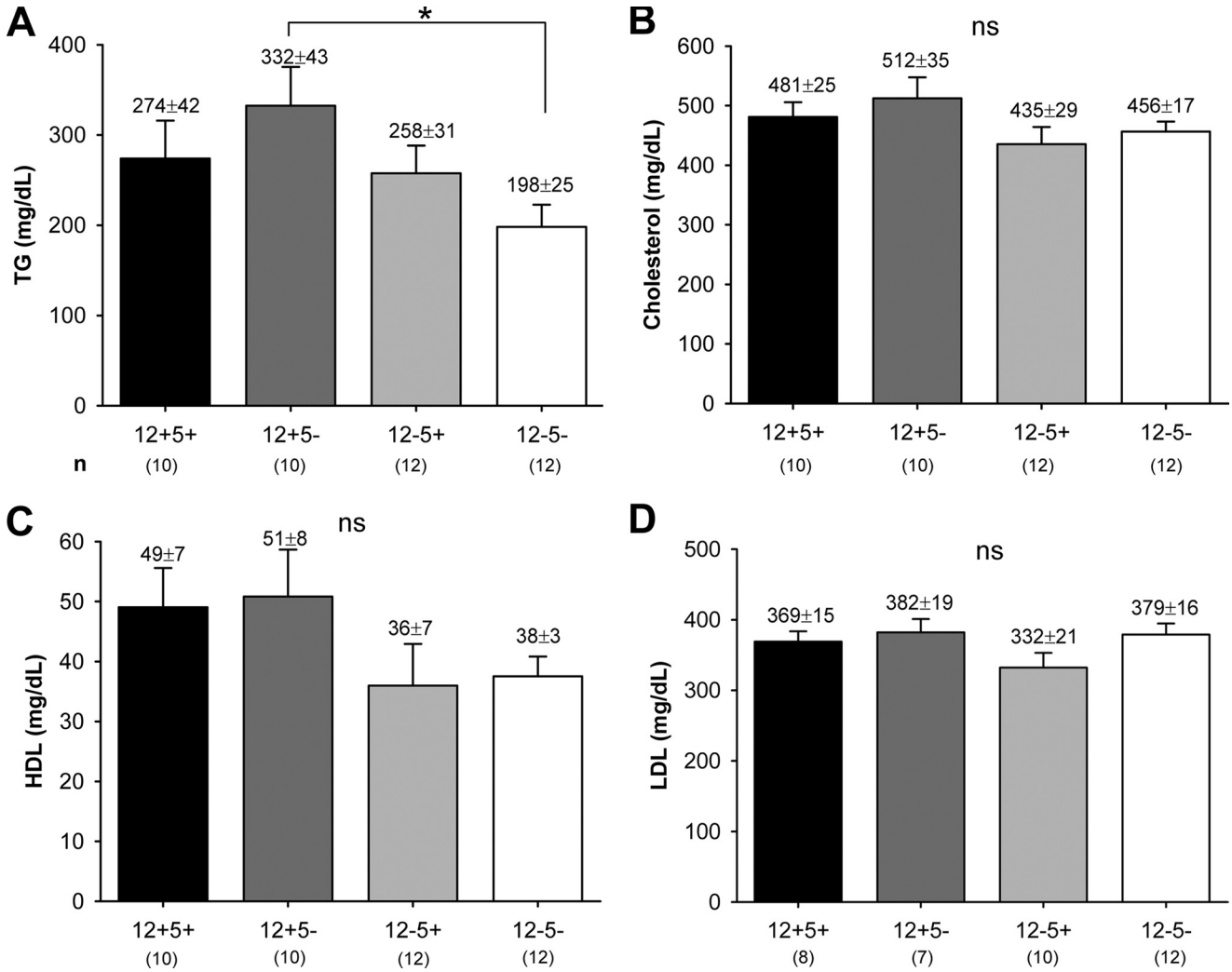

FIGURE 7. **Serum triglyceride and total/HDL/LDL cholesterol levels.** Serum was collected from healthy untreated mice of both genders and analyzed for TGs (*A*) and total (*B*), HDL (*C*), and LDL (*D*) cholesterol. Data are expressed as mean ± S.E. in mg/dl. The number of independent samples (*n*) is indicated in the figure. *, $p < 0.05$; *ns*, not significant.

determined because lipoxins were not detected in activated macrophages (see below).

Using sophisticated liquid chromatography-tandem mass spectrometry technology (40, 41), we assessed the consequences of dual 12/15-LO and 5-LO inactivation in the presence/absence of pharmacological COX-1 inhibition on cellular eicosanoid biosynthesis from endogenous AA in res-PMΦ. Drug inhibition of both LO enzymes in the context of atherosclerosis has been considered (3, 42), and macrophage-derived foam cells are the major inflammatory cell type in these lesions. Stimulation of PMΦ by calcium ionophore A23187 releases AA predominantly via cytosolic phospholipase A_2, allowing metabolism by 12/15-LO, 5-LO, and COX-1 (COX-2 is not present in unstimulated res-PMΦ (43)) or reacylation into phospholipids (44). Our data suggest that conversion of AA by 12/15-LO is more efficient than metabolism via 5-LO or COX-1 because 12/15-LO inactivation, leads to elevated free AA levels, which are elevated in the presence of COX-1 inhibition (Fig. 4*A*). This is noteworthy because 12/15-LO does not apparently translocate to the nuclear membrane (16) where most AA is released (supplemental Fig. 1 and Ref. 13). However, intra- and even intercellular shuttling of AA, which could facilitate utilization at other membrane sites, is common (45). Suicide inactivation (46, 47) and/or differences in subcellular localization might also account for the less efficient metabolism of AA by 5-LO and COX-1 compared with 12/15-LO. Remarkably with all three enzymes blocked, the concentration of free AA rises 90-fold, demonstrating that cytosolic phospholipase A_2 keeps releasing AA irrespective of intact functional coupling to downstream enzymatic pathways. This accumulation occurs despite presumably intact reacylation pathways (44), indicating that the acylation reactions are either not enhanced or already saturated. Notably in stimulated primary neutrophils, inhibition of reacylation by thimerosal drastically increases free AA levels (48).

Substrate shunting occurs from COX-1 to the 12/15-LO or 5-LO pathways and from 12/15-LO to 5-LO, which was observed previously (12), but not from 5-LO to 12/15-LO (see Fig. 4, *H* and *J*). Phorbol myristate acetate-primed, ionophore-activated wt MΦ synthesized greater quantities of LTC_4 relative to 5-HETE or LTB_4 (Fig. 4, *D–F*). LTC_4 synthase appears to function at saturating conditions because LTC_4 levels remained

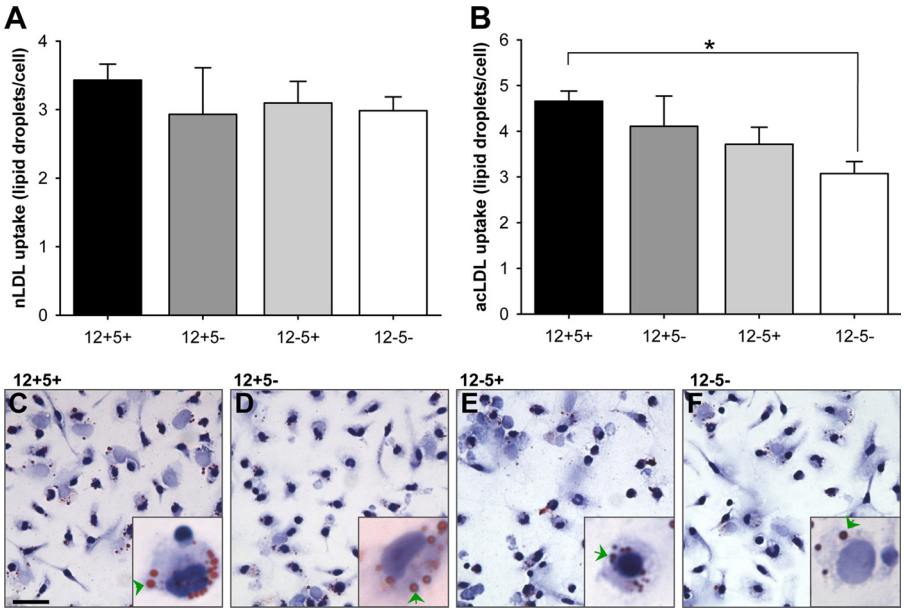

FIGURE 8. **Lipoprotein uptake by resident peritoneal macrophages.** Res-PMΦ, cultured in 8-well slides for 1.5 h, were exposed to nLDL (100 μg/ml) or AcLDL (40 μg/ml) in minimal medium for 24 h. MΦ with ≥1 lipid droplet were defined as positive, and the number of medium sized (diameter, 1–2 μm) lipid droplets was calculated per positive cell. Incidence of positive cells was ≅20% for nLDL-treated cells and ≅80% for AcLDL-treated cells. *A* shows nLDL uptake, and *B* shows AcLDL uptake, given as mean ± S.E. Representative micrographs of MΦ exposed to AcLDL including high resolution *insets* are shown (*C–F*); for all $n = 3$. *Arrowheads* point to some of the lipid droplets inside cells. *, $p < 0.05$. *Scale bar*, 25 μm.

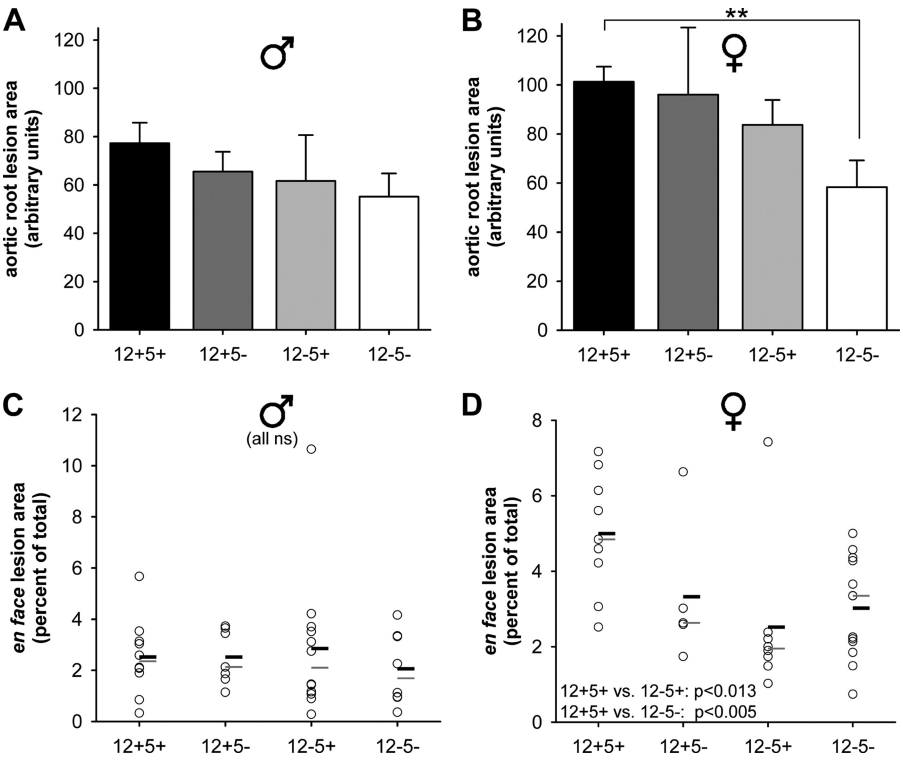

FIGURE 9. **Dual LO deficiency attenuates atherosclerotic lesion development in female mice.** Aortic root sections and entire aortae were prepared from 6-month ± 2-week-old healthy mice. *A* and *B*, averaged total lesion area of three to four cryosections per mouse stained with Oil Red O and presented as arbitrary units of male (♂) (*A*) and female (♀) (*B*) sections ($n = 8$–9/genotype; **, $p < 0.01$). *C* and *D*, fixed aortae were stained with Sudan IV, and the en face lesion area relative to the total aortic area was determined. The relative lesion area for male (*C*) and female (*D*) mice is shown, including statistical means (*thick black bars*) and medians (*thin gray bars*); $n = 7$–13. Statistical results for female mice are given in *D*. No significant differences were found for male mice (*C*). *ns*, not significant.

constant when free AA levels rose in 12−5+ cells (Fig. 4, *A* and *F*). Meanwhile the direct 5-LO products 5-HETE and LTA_4 (detected as non-enzymatic LTB_4 isomers in Fig. 4*J*) as well as LTB_4 (derived from LTA_4 hydrolase) increased under the same conditions (Fig. 4*E*). 5,6-diHETE was shown to be solely dependent on 5-LO activity and, presumably, its precursor 5-hydroperoxyeicosatetraenoic acid (Fig. 4*J*). 5,15-diHETE was only detectable in wt cells, indicating that both 12/15-LO and 5-LO are required for its biosynthesis. These diHETEs act as potential chemotactic mediators (8, 9, 39). No lipoxins were formed by a pure MΦ population in our experimental conditions, which may reflect the need for additional cell types (*e.g.* neutrophils) enabling transcellular metabolism to generate lipoxins (39, 49). Unexpectedly several 5,12-diHETE isomers were detected in 12+5− cells (Fig. 4*J*) indicating that some of these detected products might represent isoleukotrienes that originated from free radical action on phospholipids (50). However, this finding was not reproduced in dual LO-deficient cells. Further experimentation will be required to resolve this phenomenon.

11-HETE was confirmed as a clear COX-1 product (Fig. 4*G*) resulting from incomplete COX catalysis (51). COX-1 also contributed to 15-HETE, but not 12-HETE, production (Figs. 3 and 4, *H* and *I*) as illustrated by two facts. First, substantial 15-HETE was formed in dual LO-deficient cells. Second, in COX-1-inhibited wt and 12+5− cells, 15-HETE did not increase as much as 12-HETE, indicating that COX-1 forms a portion of 15-HETE in 12/15-LO-positive cells. 15-HETE is thought to escape the COX-mediated metabolism of AA (52).

Dual 12/15-LO- and 5-LO-deficient mice showed no obvious developmental or breeding abnormalities. Their serum lipid levels were within expected ranges for atherosclerosis-prone $apoE^{-/-}$

mice (Fig. 7 and Refs. 23 and 34). Of the four genotypes studied, strains lacking 5-LO showed a relatively greater incidence of cutaneous xanthomas/dermatitis (≅35 *versus* 23% in 5-LO$^{+/+}$ strains; Fig. 5*C*), a common condition in apoE$^{-/-}$ mice of the C57BL/6 genetic background (25). In contrast, strains lacking 12/15-LO displayed increased spleen to body weight ratios (Fig. 5*A*), which had previously been related to the development of myeloproliferative disorders and leukemia (32). Nonetheless the spleen enlargement observed in our studies was only moderate, although the mice we studied were on average twice as old (20–24 *versus* 10–12 weeks in Ref. 32) and were bred on an apoE$^{-/-}$ background. Thus, in accordance with a recent study (38), we were unable to confirm the severe phenotype of myeloproliferative disorder in 12/15-LO$^{-/-}$ mice.

The roles of 12/15-LO and 5-LO in atherosclerosis have been examined quite extensively over recent years (2, 3, 20, 21, 23, 24, 26). Initial studies using 12/15-LO-deficient mice indicated a clear proatherogenic role for this enzyme as shown by significantly reduced lesion areas in several models of atherosclerosis (20, 26). However, contrasting findings have been reported using different models and species (53), and recent studies indicate divergence in results in 12/15-LO-deficient mice that could be attributable to anti-inflammatory and proresolving lipid mediators (10, 54, 55). Similar mixed atherogenesis results with 5-LO gene-disrupted mice have also been reported (3, 21, 23, 24). In murine advanced lesions, 5-LO^{+} macrophages are present mainly in the adventitia rather than the intima (24) in contrast to advanced human lesions that develop over decades and contain abundant 5-LO^{+} cells in the tunica intima (56). Therefore, we studied whether some of the capricious results in atherosclerotic lesion studies could be attributable to variable eicosanoid profiles of proinflammatory *versus* anti-inflammatory AA metabolites based on our macrophage incubations in the presence or absence of one or two LO genes.

In relation to recent findings emphasizing gender-related effects of 5-LO preactivation (57), we analyzed atherosclerotic lesions in the four genotypes separated by gender. Male mice developed relatively few atherosclerotic lesions throughout the aorta and were virtually unaffected by any LO deficiency (Fig. 9, *A* and *C*). Female mice expressing both LO enzymes showed more lesions than males, consistent with previous data in apoE-deficient mice (58), and this increased burden was reduced to male levels in females lacking 12/15-LO (Fig. 9, *B* and *D*). How 12/15-LO is mechanistically involved in atherogenesis in female, but not in male, mice is presently unclear. Gender-related studies addressing the subcellular localization (corresponding to a potential preactivation state of the enzyme), as performed for 5-LO (57), have not yet been conducted with respect to 12/15-LO. Although 5-LO deficiency did not further decrease lesion size in 12/15-LO-deficient mice by en face analysis, a synergistic effect was apparent by aortic root lesion analysis (Fig. 9*B*). Disparities in 5-LO expression as well as growth dynamics and composition of atherosclerotic lesions at different sites of the aorta are well appreciated (21, 24, 59, 60), providing a possible explanation for divergent results regarding 5-LO involvement in atherosclerotic lesion development. Overall dual deficiency for 12/15-LO and 5-LO appears to be atheroprotective in female but not in male mice. These results were corroborated by *in vitro* LDL uptake experiments. Thus, dual LO-deficient res-PMΦ displayed a defect in modified LDL uptake, the first step toward foam cell formation (Fig. 8).

In summary, novel dual 12/15-LO- and 5-LO-deficient mice were generated and characterized. Interesting patterns of altered AA metabolism were observed in macrophages that could potentially explain the attenuated peritonitis and atherosclerotic lesion development in these mice. Our results provide the rationale for more detailed studies addressing dual lipoxygenase inhibitors in models of inflammation and cardiovascular disease.

Acknowledgments—We thank Laurel Ballantyne, Tim St. Amand, and Jalna Meens for expert technical assistance and Dr. Keith R. Brunt for technical assistance and helpful discussions.

REFERENCES

1. Funk, C. D. (2001) *Science* **294,** 1871–1875
2. Kühn, H., and O'Donnell, V. B. (2006) *Prog. Lipid Res.* **45,** 334–356
3. Zhao, L., and Funk, C. D. (2004) *Trends Cardiovasc. Med.* **14,** 191–195
4. Brash, A. R. (1999) *J. Biol. Chem.* **274,** 23679–23682
5. Kuhn, H., and Thiele, B. J. (1999) *FEBS Lett.* **449,** 7–11
6. Funk, C. D., Chen, X. S., Kurre, U., and Griffis, G. (1995) *Adv. Prostaglandin Thromboxane Leukot. Res.* **23,** 145–150
7. Moos, M. P., and Funk, C. D. (2008) *Trends Cardiovasc. Med.* **18,** 268–273
8. Conrad, D. J. (1999) *Clin. Rev. Allergy Immunol.* **17,** 71–89
9. Serhan, C. N. (2007) *Annu. Rev. Immunol.* **25,** 101–137
10. Serhan, C. N., Yang, R., Martinod, K., Kasuga, K., Pillai, P. S., Porter, T. F., Oh, S. F., and Spite, M. (2009) *J. Exp. Med.* **206,** 15–23
11. Huo, Y., Zhao, L., Hyman, M. C., Shashkin, P., Harry, B. L., Burcin, T., Forlow, S. B., Stark, M. A., Smith, D. F., Clarke, S., Srinivasan, S., Hedrick, C. C., Praticò, D., Witztum, J. L., Nadler, J. L., Funk, C. D., and Ley, K. (2004) *Circulation* **110,** 2024–2031
12. Sun, D., and Funk, C. D. (1996) *J. Biol. Chem.* **271,** 24055–24062
13. Luo, M., Flamand, N., and Brock, T. G. (2006) *Biochim. Biophys. Acta* **1761,** 618–625
14. Mandal, A. K., Jones, P. B., Bair, A. M., Christmas, P., Miller, D., Yamin, T. T., Wisniewski, D., Menke, J., Evans, J. F., Hyman, B. T., Bacskai, B., Chen, M., Lee, D. M., Nikolic, B., and Soberman, R. J. (2008) *Proc. Natl. Acad. Sci. U.S.A.* **105,** 20434–20439
15. Rådmark, O., Werz, O., Steinhilber, D., and Samuelsson, B. (2007) *Trends Biochem. Sci.* **32,** 332–341
16. Miller, Y. I., Chang, M. K., Funk, C. D., Feramisco, J. R., and Witztum, J. L. (2001) *J. Biol. Chem.* **276,** 19431–19439
17. Taylor, P. R., Martinez-Pomares, L., Stacey, M., Lin, H. H., Brown, G. D., and Gordon, S. (2005) *Annu. Rev. Immunol.* **23,** 901–944
18. Chen, X. S., Sheller, J. R., Johnson, E. N., and Funk, C. D. (1994) *Nature* **372,** 179–182
19. Hansson, G. K., Robertson, A. K., and Söderberg-Nauclér, C. (2006) *Annu. Rev. Pathol.* **1,** 297–329
20. Funk, C. D., and Cyrus, T. (2001) *Trends Cardiovasc. Med.* **11,** 116–124
21. Mehrabian, M., Allayee, H., Wong, J., Shi, W., Wang, X. P., Shaposhnik, Z., Funk, C. D., Lusis, A. J., and Shih, W. (2002) *Circ. Res.* **91,** 120–126
22. Subbarao, K., Jala, V. R., Mathis, S., Suttles, J., Zacharias, W., Ahamed, J., Ali, H., Tseng, M. T., and Haribabu, B. (2004) *Arterioscler. Thromb. Vasc. Biol.* **24,** 369–375
23. Cao, R. Y., St Amand, T., Gräbner, R., Habenicht, A. J., and Funk, C. D. (2009) *Atherosclerosis* **203,** 395–400
24. Zhao, L., Moos, M. P., Gräbner, R., Pédrono, F., Fan, J., Kaiser, B., John, N., Schmidt, S., Spanbroek, R., Lötzer, K., Huang, L., Cui, J., Rader, D. J., Evans, J. F., Habenicht, A. J., and Funk, C. D. (2004) *Nat. Med.* **10,** 966–973
25. Moghadasian, M. H., McManus, B. M., Nguyen, L. B., Shefer, S., Nadji, M., Godin, D. V., Green, T. J., Hill, J., Yang, Y., Scudamore, C. H., and Frohlich, J. J. (2001) *FASEB J.* **15,** 2623–2630

26. Cyrus, T., Witztum, J. L., Rader, D. J., Tangirala, R., Fazio, S., Linton, M. F., and Funk, C. D. (1999) *J. Clin. Investig.* **103,** 1597–1604
27. Smith, C. J., Zhang, Y., Koboldt, C. M., Muhammad, J., Zweifel, B. S., Shaffer, A., Talley, J. J., Masferrer, J. L., Seibert, K., and Isakson, P. C. (1998) *Proc. Natl. Acad. Sci. U.S.A.* **95,** 13313–13318
28. Havel, R. J., Eder, H. A., and Bragdon, J. H. (1955) *J. Clin. Investig.* **34,** 1345–1353
29. Basu, S. K., Goldstein, J. L., Anderson, G. W., and Brown, M. S. (1976) *Proc. Natl. Acad. Sci. U.S.A.* **73,** 3178–3182
30. Turchyn, L. R., Baginski, T. J., Renkiewicz, R. R., Lesch, C. A., and Mobley, J. L. (2007) *Comp. Med.* **57,** 574–580
31. Ross, R. (1999) *N. Engl. J. Med.* **340,** 115–126
32. Middleton, M. K., Zukas, A. M., Rubinstein, T., Jacob, M., Zhu, P., Zhao, L., Blair, I., and Puré, E. (2006) *J. Exp. Med.* **203,** 2529–2540
33. Doherty, N. S., Poubelle, P., Borgeat, P., Beaver, T. H., Westrich, G. L., and Schrader, N. L. (1985) *Prostaglandins* **30,** 769–789
34. Zhang, S. H., Reddick, R. L., Piedrahita, J. A., and Maeda, N. (1992) *Science* **258,** 468–471
35. Sendobry, S. M., Cornicelli, J. A., Welch, K., Grusby, M. J., and Daugherty, A. (1998) *J. Immunol.* **161,** 1477–1482
36. Heydeck, D., Thomas, L., Schnurr, K., Trebus, F., Thierfelder, W. E., Ihle, J. N., and Kühn, H. (1998) *Blood* **92,** 2503–2510
37. Byrum, R. S., Goulet, J. L., Snouwaert, J. N., Griffiths, R. J., and Koller, B. H. (1999) *J. Immunol.* **163,** 6810–6819
38. Dioszeghy, V., Rosas, M., Maskrey, B. H., Colmont, C., Topley, N., Chaitidis, P., Kühn, H., Jones, S. A., Taylor, P. R., and O'Donnell, V. B. (2008) *J. Immunol.* **181,** 6514–6524
39. Serhan, C. N., Chiang, N., and Van Dyke, T. E. (2008) *Nat. Rev. Immunol.* **8,** 349–361
40. Murphy, R. C., Barkley, R. M., Zemski Berry, K., Hankin, J., Harrison, K., Johnson, C., Krank, J., McAnoy, A., Uhlson, C., and Zarini, S. (2005) *Anal. Biochem.* **346,** 1–42
41. Gijón, M. A., Zarini, S., and Murphy, R. C. (2007) *J. Lipid Res.* **48,** 716–725
42. Funk, C. D. (2005) *Nat. Rev. Drug Discov.* **4,** 664–672
43. Yu, Y., Fan, J., Chen, X. S., Wang, D., Klein-Szanto, A. J., Campbell, R. L., FitzGerald, G. A., and Funk, C. D. (2006) *Nat. Med.* **12,** 699–704
44. Gijón, M. A., Riekhof, W. R., Zarini, S., Murphy, R. C., and Voelker, D. R. (2008) *J. Biol. Chem.* **283,** 30235–30245
45. Neufeld, E. J., Majerus, P. W., Krueger, C. M., and Saffitz, J. E. (1985) *J. Cell Biol.* **101,** 573–581
46. Fitzpatrick, F. A., and Soberman, R. (2001) *J. Clin. Investig.* **107,** 1347–1351
47. Rådmark, O. (2002) *Prostaglandins Other Lipid Mediat.* **68–69,** 211–234
48. Zarini, S., Gijón, M. A., Folco, G., and Murphy, R. C. (2006) *J. Biol. Chem.* **281,** 10134–10142
49. Zarini, S., Gijón, M. A., Ransome, A. E., Murphy, R. C., and Sala, A. (2009) *Proc. Natl. Acad. Sci. U.S.A.* **106,** 8296–8301
50. Harrison, K. A., and Murphy, R. C. (1995) *J. Biol. Chem.* **270,** 17273–17278
51. Randall, R. W., Eakins, K. E., Higgs, G. A., Salmon, J. A., and Tateson, J. E. (1994) *Agents Actions* **43,** 176–178; discussion 167
52. Thuresson, E. D., Lakkides, K. M., and Smith, W. L. (2000) *J. Biol. Chem.* **275,** 8501–8507
53. Shen, J., Herderick, E., Cornhill, J. F., Zsigmond, E., Kim, H. S., Kühn, H., Guevara, N. V., and Chan, L. (1996) *J. Clin. Investig.* **98,** 2201–2208
54. Merched, A. J., Ko, K., Gotlinger, K. H., Serhan, C. N., and Chan, L. (2008) *FASEB J.* **22,** 3595–3606
55. Serhan, C. N., Yacoubian, S., and Yang, R. (2008) *Annu. Rev. Pathol.* **3,** 279–312
56. Spanbroek, R., Grabner, R., Lotzer, K., Hildner, M., Urbach, A., Ruhling, K., Moos, M. P., Kaiser, B., Cohnert, T. U., Wahlers, T., Zieske, A., Plenz, G., Robenek, H., Salbach, P., Kuhn, H., Radmark, O., Samuelsson, B., and Habenicht, A. J. (2003) *Proc. Natl. Acad. Sci. U.S.A.* **100,** 1238–1243
57. Pergola, C., Dodt, G., Rossi, A., Neunhoeffer, E., Lawrenz, B., Northoff, H., Samuelsson, B., Rådmark, O., Sautebin, L., and Werz, O. (2008) *Proc. Natl. Acad. Sci. U.S.A.* **105,** 19881–19886
58. van Ree, J. H., van den Broek, W. J., Dahlmans, V. E., Groot, P. H., Vidgeon-Hart, M., Frants, R. R., Wieringa, B., Havekes, L. M., and Hofker, M. H. (1994) *Atherosclerosis* **111,** 25–37
59. VanderLaan, P. A., Reardon, C. A., and Getz, G. S. (2004) *Arterioscler. Thromb. Vasc. Biol.* **24,** 12–22
60. Gown, A. M., Tsukada, T., and Ross, R. (1986) *Am. J. Pathol.* **125,** 191–207